THE JOURNAL OF PHYSICAL CHEMISTRY B

ARTICLE

pubs.acs.org/JPCB

Molecular Mixture as an Effective Single-Component System

Ryan J. Larsen* and Charles F. Zukoski

Department of Chemical and Biomolecular Engineering, University of Illinois at Urbana−Champaign, 114 Roger Adams Laboratory, 600 South Mathews Avenue, Urbana, Illinois 61801, United States

ABSTRACT: Colloidal systems exhibit a dramatic slowdown in particle dynamics at high concentrations. The study of the concentration-induced glass transition in these systems has been greatly simplified by treating the colloidal phase as an effective single component in a viscous continuum. We seek to apply an effective single-component approach to molecular systems by investigating a material that also exhibits a dramatic slowdown as the relative concentration of two components change. Our system is a binary mixture of ethanol and citric acid, in which the size ratio of the particles is 0.7. We measure the temperature and concentration dependence of the self-diffusivity of both components using pulse-gradient NMR. We model our data with an elementary free volume model and show that the self-diffusivity of both components depends on the properties of an effective single component. The particle size of the effective single component is the number-averaged size of the two components. Our results demonstrate that mixtures can be used to study the effect of particle size on glassy dynamics and are therefore useful for understanding systems that are intermediate between molecular and colloidal.

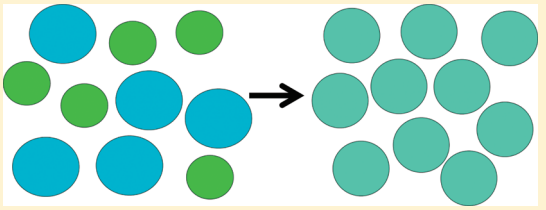

I. INTRODUCTION

The glass transition is a general phenomenon that occurs in a wide variety of materials. The study of the glass transition is complicated by the fact that it is sensitive to several factors, including the attractions between particles,[1] crowding effects, valence,[2] and deformability of the glass-forming particles.[3] The respective roles of these effects can be elucidated by comparing various routes by which the glass transition is approached. For example, the dependence of the relaxation time on the density of molecules can differ dramatically when the glass transition is approached under isothermal or isobaric conditions,[4,5] and this difference can be attributed to the effect of attractions between particles.[6]

Although the glass transition is commonly approached by changing the temperature or pressure, it is also possible to approach the glass transition by tuning the relative concentration of two phases. This is commonly done in colloidal systems; the concentration of the colloidal phase can be continuously increased until a glass is formed.[7,8] Concentration-induced glass transitions are also observed in a variety of molecular systems. For example, the concentration of water, a comparatively small molecule, is a critical factor for determining the glassy behavior of food products and pharmaceuticals.[9,10] Small molecules and nanoparticles are commonly used as plasticizers in polymer melts.[11,12] In these systems the dynamics of the mixture depend on the relative concentration of large and small molecules. In general, glassy behavior is induced as the concentration of the large particles increases relative to the small particles.

Concentration-induced transitions are not limited to glass transitions and can also include liquid−liquid phase transitions and gel formation.[13] Although such phase behavior can be sensitive to the details of the molecules,[14] a basic understanding of the mechanisms associated with these transitions can be can be achieved from studies of hard-sphere systems.[1,2,15−18]

In the case of binary mixtures of hard spheres of size ratio q, entropic effects alone can give rise to phase separation and gel formation when q is sufficiently small.[15,17−19] By contrast, for q sufficiently close to unity, systems can exhibit a simultaneous arrest of both phases or formation of a double glass. For these systems, mode coupling theory (MCT) has been used to determine values of the combined volume fraction, ϕ_m, where the system transitions to a state where the dynamics are dominated by cooperative phenomena.[20] When ϕ_m exceeds a crossover volume fraction, ϕ_{mc}, the dynamics of localized particles are inhibited by nearest neighbors and relaxation requires activated hopping of particles between nearest neighbor cages.[21,22] For binary mixtures of hard spheres of q between 0.7 and unity, values of $\phi_{mc} \approx 0.516$ are roughly independent of the relative concentration of the two species.[20] A similar trend is observed in measurements of the combined volume fractions at random close packing, ϕ_{mr}, of binary mixtures. For size ratios between 0.7 and unity, values of $\phi_{mr} \approx 0.64$ are roughly independent of the relative concentration of the two species.[23] This observation can be rationalized on geometrical grounds: for $0.7 < q < 1.0$, the smaller particles are not sufficiently small to fit within the interstices formed by a close-packed arrangement of large particles. Therefore, the mixtures of particles pack with the same efficiency as the monodisperse hard spheres.[23] Mixing two close-packed systems of monodisperse spheres of $0.7 < q < 1.0$ to

Received: December 20, 2010
Revised: February 19, 2011
Published: March 18, 2011

produce a close-packed mixture does not create or reduce the free volume, and the mixing is therefore ideal.

These observations have been used to rationalize the fact that binary alloys of liquid metal for which $0.7 < q < 1.0$ generally exhibit ideal mixing whereas those of size ratio less than 0.7 generally do not.[23] For binary hard-sphere systems of $0.7 < q < 1.0$, values of $\phi_{mc} \approx 0.516$ and $\phi_{mr} \approx 0.64$ bracket a region in which the dynamics dramatically slow down as ϕ_m increases. The combined volume fraction, ϕ_{gm}, at the glass transition is expected to lie between these limits. The glass transition is generally assigned to occur when the time scale of particle rearrangement reaches a value that is set by a convention that is practical yet arbitrary.[1]

Results from binary systems suggest the possibility of realizing a binary system in which a concentration-dependent transition to glassy dynamics is governed by an ideal, or linear, combination of two components. In this paper we probe such a transition and show that because of its ideal characteristics the dynamics of both components depend on the properties of an effective single component, which is a weighted average of the two single components. Our results show that a molecular mixture provides an experimental approximation of a conceptually simple, yet physically unrealizable, approach to the glass transition: a continuous change in the size and strength of attraction of the particles in a single-component system.

Our experiments are performed on a mixture of two species of size ratio $q \approx 0.7$: citric acid (CA) and ethanol (EtOH). Although the difference in the molecular sizes is not great, the glass transition temperatures of the two materials differ considerably: $T_g = 11$ °C for CA[24] and −178 °C for EtOH.[25] Because of the large separation in T_g, we are able to prepare materials that exhibit a wide range of dynamical behavior, from liquid to glassy, at constant pressure and temperature, simply by increasing the concentration of CA. In this manner the system qualitatively resembles a colloidal system, despite the fact that the CA molecules are well below the size range of nanometer to micrometer that is generally associated with colloidal particles.

We characterize the dynamics of this system by measuring concentration dependence of the self-diffusivity using the NMR techniques. We model the system by using an elementary free volume model,[11] the Gordon−Taylor equation for mixtures,[26] and a Carnahan−Starling equation of state with a van der Waals term added to it.[27,28] Each of these approaches can be used to relate the dynamics of both of the components to an effective single-component system that is characterized by properties that are intermediate between those of the two single components.

II. EXPERIMENTAL SECTION

Citric acid (CA) and ethanol (EtOH) can be mixed in a wide range of ratios to form a clear liquid, or glass, in which crystallization does not occur for several hours. At room temperature CA is a crystal; it exhibits a melting point at 153 °C.[29] When liquids of CA are cooled to room temperature, they are close to their glass transition point, 11 °C, and form a solid-like material. When the cooling is repeated on solutions with increasing concentrations of EtOH, the liquid formed at room temperature becomes progressively less viscous. As the concentration of CA decreases to zero, the viscosity of the solution approaches that of ethanol. The combination of CA and EtOH therefore provides an approach to glassy behavior that is concentration dependent.

Our samples were prepared using anhydrous citric acid as received from Sigma and USP grade 200 Proof absolute Ethyl Alcohol from AAPER, Pharmco and AAPER, and Decon Laboratories, Inc. For samples of the weight fraction of CA, w_2, the CA could be dissolved at room temperature by stirring. For samples of higher w_2, it was necessarily to heat the samples to form a solution. This was done at temperatures between 90 and 140 °C for 3−10 min, until the suspension turned clear. In some of the samples used for the density measurements, moderate boiling was observed. We performed weight measurements afterward to quantify the loss, assuming that only ethanol was lost. Experiments were performed within several hours, typically before any crystallization was observed.

Density Measurements. The density, ρ, of solutions of various concentrations of CA in EtOH was measured using a DA-100 Density/Specific Gravity Meter (Mettler/KEM).

Measurement of Self-Diffusivity Using Nuclear Magnetic Resonance (NMR). The long-time self-diffusivity of both CA and EtOH was measured using a 1H Pulse Gradient Spin Echo (PGSE) NMR with a 600 MHz spectrometer (Varian Unity Inova 600). The PGSE experiment consists of a spin echo experiment in which the magnitude of the signal is sensitized to the diffusion by applying a pair of gradient pulses of magnitude g and duration δ before and after the 180° rf pulse that is responsible for the formation of the spin echo. Molecular diffusion that occurs during the time Δ between application of the two gradient pulses causes the spins to dephase and gives rise to an attenuation in the magnitude, S, of the signal of the echo. In the PGSE experiment, the pulse sequence is repeated for various values of g and the attenuation of the signal as a function of g is related to the self-diffusivity, D, with the relation

$$S(g)/S(0) = \exp[-\gamma^2 g^2 \delta^2 D(\Delta - \delta/3)] \qquad (1)$$

where γ is the gyromagnetic ratio of hydrogen.[30,31]

We performed PGSE experiments by first injecting our samples into a spherical bulb microcell (Wilmad Glass, 5 mm), which was then inserted into an NMR tube (Wilmad Glass, 5 mm) filled with deuterium oxide (Aldrich, 99.9%). The advantage of this approach is that the signal originates only from the sample within the bulb. This minimizes errors due to any nonlinearities in the pulsed magnetic field gradients. We verified the consistency of our approach by measuring values for the self-diffusivity of water that were independent of both Δ and the duration δ of the gradient pulses. The most consistent results were obtained when values of g were maintained between 5 and 50 G/cm. Therefore, this range of g values was used in all of our calibrations and experiments. We also verified that we were able to obtain consistent values of self-diffusivity using both the PSGE experiment and the stimulated PGSE experiment, in which the 180° pulse is split into two 90° pulses, so that the magnetization is stored in the longitudinal direction, thereby diminishing the attenuation of the signal due to relaxation of the transverse magnetization.[32]

Prior to each set of experiments, we measured the self-diffusivity of water at the same temperature at which the experiments were to be performed and calibrated g by comparing the measurements to literature values of self-diffusivity.[33] The experiments were performed at 9, 25, and 50 °C, with Δ = 300−400 ms. The delay time between the gradient sequences was 15 s or greater. We verified that changing the delay time between 15 and 30 s did not affect our results.

We were able to measure the diffusion coefficient of both components in the mixture. This was possible because the Fourier transform (FT) of the signal gives rise to distinct peaks, characteristic of the chemical shift associated with the hydrogen atoms in each species. A diffusion coefficient associated with each peak, or cluster of peaks, was calculated by repeating a stimulated PGSE pulse sequence eight times while varying g between 5 and 50 G/cm. For each component of the mixture, we tuned δ so that the amplitude of the peaks associated with that component would decay to approximately 5−20% of the initial value. We then measured $S(g)$ for each peak by integrating the FT using software provided by the manufacturer of the spectrometer. Using these values we calculated D and the associated uncertainty by performing a linear fit to measured values of $\log(S(g)/S(0))$ as a function of $(-\gamma^2 g^2 \delta^2(\Delta - \delta/3))$. For CA, we calculated the diffusion coefficient by integrating over a single cluster of peaks located near 2 ppm. For EtOH in the absence of CA, three distinct peaks are located at 1, 3, and 4 ppm. These correspond to the chemical groups CH_3, CH_2, and OH, respectively. In the absence of CA, the diffusion coefficients measured from all three peaks are the same. As the concentration of CA increases, the apparent diffusion coefficient measured from the peak associated with the OH group became progressively lower than the apparent diffusion coefficients measured from the other two peaks. This difference was greatest at the maximum value of w_2 = 0.41. For this sample, the apparent diffusion coefficient measured from the peak associated with the OH group was 45% lower than that measured from the other peaks. We expect that this occurs because some of the signal associated with this peak originates from the OH groups present on the CA molecules. We therefore calculate the self-diffusivity of the EtOH molecule using the average of the diffusion coefficients calculated from the peaks associated with CH_2 and CH_3.

A second complication associated with our measurements of high CA concentration is that the EtOH peak associated with the CH_2 group (near 3 ppm) overlapped somewhat with the cluster of peaks used to measure the self-diffusivity of CA. However, because the self-diffusivity of CA is lower than that of EtOH, the peak associated with CA was more persistent when the gradient pulses were applied.[34] In the spectrum obtained from elevated values of g, in the range from 38 to 50 G/cm, we observed little or no overlap between peaks associated with different species. Values of self-diffusivity calculated from this limited range of g values were not systemically different from those calculated using the full range of g values (5−50 G/cm). The absolute value of the percent difference in the self-diffusivity obtained using both ranges of g were, on average, only 6%. This value is close to the uncertainty associated with measurements of g that were obtained using the range of 38−50 G/cm (4%). We therefore report values of the self-diffusivity of CA that are calculated using the range of 5−50 G/cm. Each reported measurement is the result of a single stimulated PGSE experiment. The variation in D associated with repeated measurements was similar to the uncertainty associated with the linear fits. Because both sources of error are approximately 5−6%, we estimate that the total uncertainty of each measurement is less than 10%.

Self-diffusivity measurements were performed at 0, 0.2, 0.31, and 0.41 wt % of CA. We prepared a sample at 0.5 wt %, but the sample crystallized before the measurements were performed. We did not perform measurements below 0.2 wt % because the size of peaks associated with CA was too small for accurate diffusion measurements.

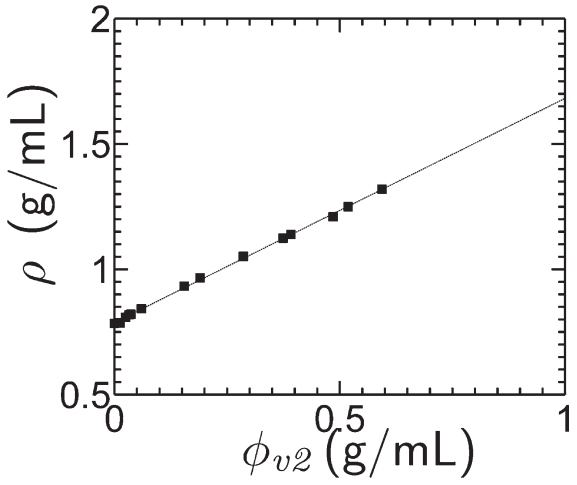

Figure 1. Density of mixtures of CA and EtOH is linear with respect the molar volume fraction of CA, ϕ_{v2}. The line is the linear fit to the data, as described in the text.

III. RESULTS

Density. We characterized the mixing volumes of CA and EtOH by performing density measurements of mixtures of CA and EtOH at 25 °C. Our results show that the density of the mixtures is linear with respect to the molar volume fraction of citric acid

$$\phi_{v2} = \frac{w_2/\rho_2}{w_2/\rho_2 + w_1/\rho_1} \quad (2)$$

as shown in Figure 1. Here we used literature values for the density of EtOH, ρ_1 = 0.7893 g/mL, and CA, ρ_2 = 1.665 g/mL, at 20 °C.[29] A linear fit to the data provides estimates of the densities of the two pure components, ρ_1 = 0.776 g/mL and ρ_2 = 1.658 g/mL. This result indicates that the molar volume of each species in the mixture is the same as the molar volume of the species in its neat form.

We rationalize our observation of ideal mixing by showing that the size ratio, q, of the binary systems is within the range of 0.7−1.0. The van der Waals or hard-core volumes, v^*, of the molecules are typically reported in terms of a van der Waals radius, r^*, through the relation $v^* = (4/3)\pi r^{*3}$. Estimates of r^* are not unique; they depend on the method of calculation.[35] We estimate r^* of both molecules in a consistent manner by using a standard molecular increment approach.[35,36] In this approach, the contributions from each atom are summed to obtain v^*, from which a van der Waals radius, r^*, is calculated. Values of $v^*$and r^* can be adjusted to account for hydrogen bonding. However, because these effects are small and because we do not know the number of hydrogen bonds formed by each species as a function of relative concentration, we neglect the effect of hydrogen bonding in our calculations of v^*. We therefore find that EtOH has a van der Waals radius of r_1^* = 2.33 Å and CA has a van der Waals radius of r_2^* = 3.31 Å.[35] Therefore, for the CA/EtOH system, $q = r_1^*/r_2^*$ = 0.71. The fact that q falls within the range of 0.7−1.0 is consistent with the fact that the two phases will mix in an ideal manner.

Self-Diffusivity. Self-diffusivity measurements show that the long time self-diffusivity D_i of each component i decreases as the temperature decreases and as the weight fraction, w_2, of

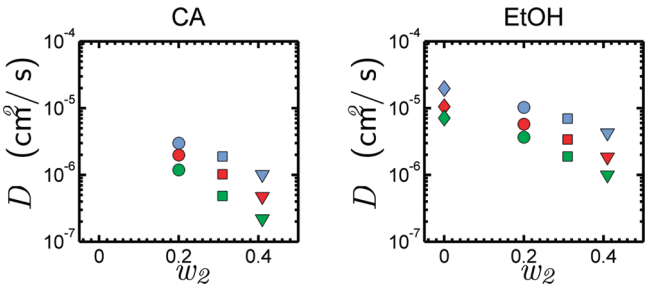

Figure 2. Self-diffusivity of CA and EtOH as a function of the weight fraction, w_2, of CA at 50 (blue symbols), 25 (red symbols), and 9 °C (green symbols).

CA increases (Figure 2). We characterize the dependence of D_i on both temperature and w_2 using the elementary free volume model. Although the elementary free volume model that we employ is not rigorous, the form of the equations suggests a facile connection between the two-component system and an effective single-component system. This connection is further developed by writing the free volume model in the form of the Vogel−Fulcher−Tammann−Hesse (VTHF) equation which is also in the form of a single-component system.[37,38] We then show that the mapping of the two-component system onto a single-component system is preserved in a simple equation of state. This provides a thermodynamic basis for the mapping of the mixture to an effective single component.

Elementary Free Volume Model. Mobility of liquid molecules requires that the liquid possesses sufficient "free volume". Free volume is not occupied by molecular cores, and it can be randomly distributed or rearranged throughout the material without giving rise to an energy penalty associated with the interpenetration of molecular cores.[39] Free volume theories relate the free volume of the liquid to transport properties, such as self-diffusivity.[16,40−43] The standard equation for the self-diffusivity of a single-component liquid is given by the Doolittle equation[44]

$$D = D_0 \exp\left(-b\frac{V^*}{V_f}\right) \tag{3}$$

where V^* is the total volume that is occupied by the molecular cores, V_f is the total free volume, and b and D_0 are constants. The Doolittle equation can be justified theoretically by calculating the probability that random fluctuations in the free volume will open up holes of a critical size in the liquid, thereby allowing particle motion to occur.[40] A variety of approaches have been used to extend free volume models to mixtures.[11,45−49] In a manner that is consistent with the simplest of these approaches,[11] we assume that the self-diffusivity, D_i, of each component i is governed by the ratio of the total free volume, V_{fm}, to the total hard-core volumes of the molecules, V^*_m, or

$$\frac{V_{fm}}{V^*_m} = \frac{N_1 v_{f1} + N_2 v_{f2}}{N_1 v^*_1 + N_2 v^*_2} \tag{4}$$

where subscripts 1 and 2 indicate the components EtOH and CA, respectively, and N_i is the number of molecules of component i.

Applying the Doolittle equation we obtain

$$D_i = D_{0i} \exp\left(-b_i\frac{V^*_m}{V_{fm}}\right) \tag{5}$$

where D_{0i} and b_i are constants that are species dependent.

In an elementary free volume theory for single components, the free volume is given by

$$V_f = N v_g[f_{fg} + \Delta\alpha(T - T_g)] \tag{6}$$

where v_g is the total volume associated with the molecule, or the molecular volume, at the glass transition, f_{fg} is the fractional free volume at the glass transition, and $\Delta\alpha$ is the difference between the coefficient of thermal expansion above and below the glass transition.[11] In a consistent manner, we take the free volume, V_{fm}, of the mixture to be a linear combination of the free volume of the two components[11]

$$V_{fm} = N_1 v_{g1}[f_{fg1} + \Delta\alpha_1(T - T_{g1})] + N_2 v_{g2}[f_{fg2} + \Delta\alpha_2(T - T_{g2})] \tag{7}$$

We simplify this expression by assuming that at the glass transition the particles are completely immobilized. According to this assumption, any volume that is "unoccupied" by particles does not contribute to the mobility of the particles and is therefore not free volume, so that $f_{fg1} = f_{fg2} = 0$. This assumption will be most accurate for high temperatures where $f_{fgi} \ll \Delta\alpha_i(T - T_{gi})$. With this assumption the equation becomes

$$V_{fm} = N_1 v_{g1}[\Delta\alpha_1(T - T_{g1})] + N_2 v_{g2}[\Delta\alpha_2(T - T_{g2})] \tag{8}$$

To apply this model to our data we estimate values of v_{gi} by assuming that the coefficient of thermal expansion at 20 °C holds for all temperatures and by extrapolating the density of each liquid to the glass transition temperature, T_{gi}, and calculating $v_{gi} = M_{wi}/(\rho_{gi}N_a)$, where M_{wi} is the molecular weight, ρ_{gi} is the extrapolated density, and N_a is the Avogadro constant. We estimate the thermal expansion coefficient, α_2, of CA by applying the relation $T_{g1}\alpha_1 = T_{g2}\alpha_2$, which has been shown to be approximately valid for a variety of glass formers.[50] Values of $\Delta\alpha_i$ are assumed be proportional to α_i, with $\Delta\alpha_i/\alpha_i = p_i$. Typical values of p_i are in the range of 0.5−0.8.[50] We assume that $p = p_1 = p_2 = 0.7$ and that the volumes, v^*_i, of the molecular cores are independent of temperature.

When $\log(D_i)$ is plotted as a function of V^*_m/V_{fm} the data obtained at different temperatures and concentrations collapse onto two parallel lines (see Figure 3). Data from EtOH collapse to the line of higher self-diffusivity than CA. Although we obtained this collapse by roughly estimating a value for α_2, our results are not sensitive to the particular value of this variable; a similar collapse can be obtained by taking $\Delta\alpha_2 = 0$. This is consistent with the fact that the glass transition temperature of CA, T_{g2}, is 11 °C, close to the temperature of our measurements, and CA contributes little to the total free volume. Although the free volume contribution from the CA molecules is small, we retain this term in our analysis for completeness and for the sake of relating our analysis to standard equations.

The collapse of the data also changes little as p_1 and p_2 are varied independently over the expected range of 0.5−0.8. For a given combination of p_1 and p_2 it is possible to calculate values of D_{0i} and b_i from the data by performing a least-squares fit to the data. Calculated values of D_{0i} and b_i fall within the expected range when p_1 and p_2 are varied over the range of 0.5−0.8. For $p = p_1 = p_2 = 0.7$, we obtain $b_1 = -1.07$, $b_2 = -1.23$ and $D_{01} = 6.6 \times 10^{-4}$, $D_{02} = 4.1 \times 10^{-4}$. The ratio b_2/b_1 is 1.15, and this result is independent of the choice of p_1 and p_2. The fact that $b_2 > b_1$ is consistent with the expectation that the critical hole size necessary for diffusion will be greater for the molecule of greater

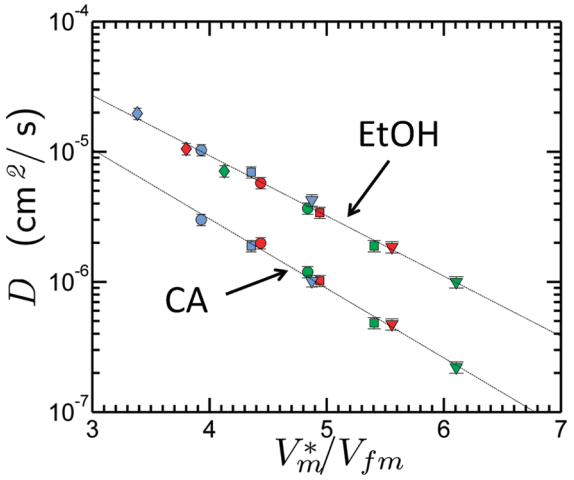

Figure 3. Self-diffusivity of both CA and EtOH collapses when plotted as a function of V_m^*/V_{fm}. The solid lines are fits to eq 5. The symbols near the upper line pertain to EtOH, and the symbols near the lower line pertain to CA. Symbols are the same as those used in Figure 2: T = 50 (blue symbols), 25 (red symbols), and 9 °C (green symbols); w_2 = 0 (diamonds), 0.2 (circles), 0.3 (squares), and 0.4 (triangles).

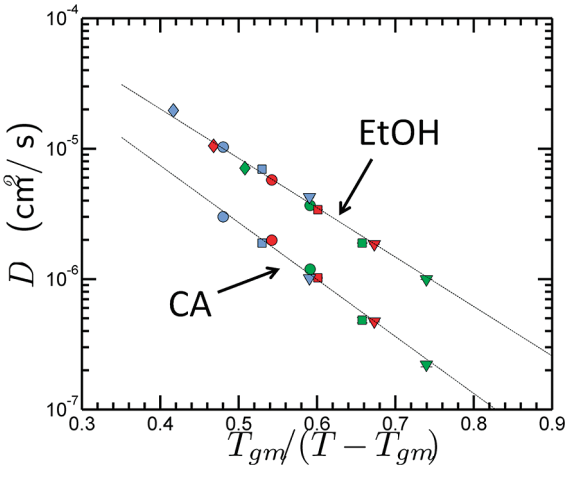

Figure 4. Self-diffusivity of both CA and EtOH collapses when plotted as a function of $T_{gm}/(T - T_{gm})$. The solid lines are obtained using values of $\bar{b}_i$ calculated from eq 15 and the same values of D_{0i} that were obtained from fitting eq 5. The symbols near the upper line pertain to EtOH, and the symbols near the lower line pertain to CA. Symbols are the same as those used in Figure 2: T = 50 (blue symbols), 25 (red symbols), and 9 °C (green symbols); w_2 = 0 (diamonds), 0.2 (circles), 0.3 (squares), and 0.4 (triangles).

size.[40,46,48,49] The differences between the two components can therefore be expressed solely in terms of the constants b_i and D_{0i}. However, the temperature and concentration dependence of the dynamics of both components are governed by the ratio V_m^*/V_{fm}. This variable is equivalent to v_m^*/v_{fm}, where $v_m^* = V_m^*/N$ and $v_{fm} = V_{fm}/N$ are the number-averaged molecular size and free volume, respectively. This suggests that the dynamics of the two-component system are governed by an effective single component of size v_m^* and molecular free volume v_{fm}.

Gordon−Taylor Equation. The ratio v_m^*/v_{fm} that determines the dynamics of both components can be modified by increasing the concentration of CA or by lowering the temperature. By assuming that the glass transition is governed by the free volume, it is possible to predict the glass transition temperature, T_{gm}, of a mixture for any given concentration of CA. To do this, we assume that the free volume at the glass transition is governed by a linear superposition of the free volumes at the glass transitions of the single components, $V_{fm}/V_m^* \approx N_1 v_{g1} f_{g1} + N_2 v_{g2} f_{g2}$. Combining this relation with eq 7, we obtain

$$T_{gm} = \frac{N_1 v_{g1} \Delta\alpha_1 T_{g1} + N_2 v_{g2} \Delta\alpha_2 T_{g2}}{N_1 v_{g1} \Delta\alpha_1 + N_2 v_{g2} \Delta\alpha_2} \tag{9}$$

The same relation also applies when f_{gi} is taken to be zero. Equation 9 can be written in the form of the Gordon−Taylor equation,[26] which has been shown to accurately predict T_{gm} of a variety of mixtures.[9] This is done by taking $N_i v_{gi} = \omega_i/\rho_{gi}$ and rearranging to obtain

$$T_{gm} = \frac{w_1 T_{g1} + K w_2 T_{g2}}{w_1 + K w_2} \tag{10}$$

where

$$K = \frac{\rho_{g1} \Delta\alpha_2}{\rho_{g2} \Delta\alpha_1} = \frac{\rho_{g1} T_{g1}}{\rho_{g2} T_{g2}} \tag{11}$$

The second expression for K is obtained using the Simha−Boyer rule[50]

$$\Delta\alpha_1 T_{g1} = \Delta\alpha_2 T_{g2} \tag{12}$$

Combining eqs 8, 9, and 12 and the relation $V_m^* = N_1 v_1^* + N_2 v_2^*$

$$\frac{V_{fm}}{V_m^*} = \Delta\alpha_1 T_{g1} \frac{(T - T_{gm})}{T_{gm}} \left(\frac{N_1 v_{g1} + N_2 v_{g2}}{N_1 v_1^* + N_2 v_2^*} \right)$$

$$= \Delta\alpha_1 T_{g1} \frac{(T - T_{gm})}{T_{gm}} \frac{1}{\phi_g} \tag{13}$$

where ϕ_g represents the volume fraction at the glass transition. Substituting eq 13 into eq 5, we obtain

$$D_i = D_{0i} \exp\left(-\bar{b}_i \frac{T_{gm}}{(T - T_{gm})} \right) \tag{14}$$

where

$$\bar{b}_i = b_i \left(\frac{\phi_g}{\Delta\alpha_1 T_{g1}} \right) \tag{15}$$

We estimate that ϕ_g varies between 0.76 and 0.77 for all values of w_2 in our experiments. We therefore take it to be a constant, ϕ_g = 0.76, so that the parameters $\bar{b}_i$ are also constants. With this simplification, eq 14 is of the same form as the Vogel−Fulcher−Tammann−Hesse (VFTH) equation.[37,38] As predicted by eq 14, measured values of D_i collapse when plotted as a function of $T_{gm}/(T - T_{gm})$, as shown in Figure 4. As with Figure 3, the figure is obtained by assuming $p = p_1 = p_2$ = 0.7. However, the collapse shown changes little as p is varied in the range of 0.5−0.8.

dx.doi.org/10.1021/jp1120838 |J. Phys. Chem. B 2011, 115, 3981–3991

It is possible to rewrite eq 14 in a form that matches the form of the Doolittle equation for a single component

$$D_i = \overline{D}_{0i} \exp\left(-b_i \frac{v_m^*}{v_{g\mathrm{eff}} \Delta\alpha_{\mathrm{eff}} (T - T_{gm})}\right) \quad (16)$$

where

$$v_{g\mathrm{eff}} = (N_1 v_{g1} + N_2 v_{g2})/N \quad (17)$$

$$\Delta\alpha_{\mathrm{eff}} = (\Delta\alpha_1 T_{g1})/T_{gm} \quad (18)$$

The particle size of the effective single-component system is given by number-averaged particle size, v_m^*. The effective thermal expansion coefficient, $\Delta\alpha_{\mathrm{eff}}$, depends on T_{gm} in a manner that is consistent with the Simha−Boyer relation (eq 12).

Although the Simha−Boyer and Gordon Taylor (eq 9) equations have been shown to be approximately valid for a variety of glass formers, they are not rigorous.[9,39] Nevertheless, these elementary equations suggest the dynamics of the mixture are controlled by an effective single component. To learn whether the effective single-component approach is compatible with a thermodynamic treatment we model the mixture by using an equation of state for a single component that has been extended to two components. We first show that the mixture can be modeled with the two-component equation of state. We then show that the mixture can also be modeled using the single-component equation of state, with effective or average properties of the single component.

Equation of State Model. The equation of state provides a thermodynamic basis for the dependence of the volume on the temperature for the individual components, their mixtures, and the effective single component. We first characterize the individual components by modeling them using the Carnahan−Starling (CS) equation of state for hard spheres with a van der Waals (vdW) attraction term added to it.[28] As with the free volume model we assume that the hard-core volume of the molecules is independent of the temperature. The repulsive forces arise solely from volume exclusion or entropic effects that are described by the Carnahan−Starling equation of state

$$\frac{p_{CS} v}{k_B T} = \frac{1 + \phi + \phi^2 - \phi^3}{(1 - \phi)^3} \quad (19)$$

where p_{CS} is the total or hard-sphere pressure, k_B is the Boltzmann constant, and ϕ is the volume fraction given by v^*/v. Here we assume that the volume, v^*, calculated from the molecular increments method is equal to the hard-sphere volume. Comparisons of values of v^* and values of the hard-sphere volume calculated by fitting eq 19 have shown that this assumption is accurate to within approximately 5% by volume for a variety of molecules.[28] In the van der Waals approach, the attractive portion of the molecular potential is sufficiently long range that it can be treated in a mean-field sense as an effective pressure, p_{eff}, using a van der Waals term, given by $p_{\mathrm{eff}} = a'/v^2 = a'\bar{\rho}^2$, where a' is a measure of the strength of attraction and $\bar{\rho}$ is the number density of particles. The total pressure is $p_{CS} = p_{\mathrm{atm}} + p_{\mathrm{eff}}$, where p_{atm} is atmospheric pressure.

We first use eq 19 to model both of the single components. We calculate values, a_i', of the single components from knowledge of ϕ_0 at 20 °C and atmospheric pressure (STP). Values of ϕ_0 are obtained from the relation v^*/v, where we obtain v from literature values of density and molar mass.

We calculate that for EtOH $\phi_{01} = 0.55$ and for CA $\phi_{02} = 0.79$. The value of ϕ_{02} for CA is greater than the maximum volume fraction, 0.74, expected for close-packed hard spheres in a crystalline lattice. This may be due to the fact that the CA molecule is not perfectly nonspherical. When hydrogen bonds form between adjacent molecules, their van der Waals volumes can effectively "overlap". This effect is accounted for by decreasing the molecular volume of each molecule and drawing flat boundaries between the molecules. The faceted shapes of the resulting molecules may allow them to pack to volume fractions that are higher than those available to hard spheres.

Although CA at STP is crystalline, we assume that in the mixture CA is a liquid state with a density given by ρ_i. This assumption is consistent with our density measurements of the CA/EtOH mixture which were performed on the liquid state. The volume fraction of CA in the liquid state is greater than the maximum random close packed (RCP) volume fraction of hard spheres, which is 0.64.[51] Values of RCP are shape dependent; slightly nonspherical particles can exhibit values of the RCP that exceed those of spheres.[52] Values of ϕ_g are expected to be less than RCP. At STP, CA is slightly above T_{g2}, which is 11 °C. We therefore surmise that the RCP of the CA molecules occurs at a volume fraction that is greater than $\phi_{02} = 0.79$. The CS equation of state diverges at the physically unrealistic value of unity. Because the CS lacks a divergence near 0.79, it may underestimate the strength of molecular attractions. The estimates of the molecular attractions that we obtain in this manner therefore represent lower bounds.

From calculated values of ϕ_0 and eq 19, we calculate $a_1 = a_2' N_a^2 = 2.58$ N m^4/mol^2 for EtOH and $a_2 = a_2' N_a^2 = 60.74$ N m^4/mol^2 for CA. Recognizing that more complicated approaches accounting for variations with temperature and pressure have been developed[28] and that detailed information on the temperature and pressure dependence of the CA density required to use these models is not available, we apply the same simple approach to both species. We find that this approach is sufficiently accurate to reproduce the trends observed in Figure 3 and to provide a thermodynamic justification for the reduction of the two-component system to an effective single component.

With these parameters, we use the CS−vdW equation to calculate the volume fraction, ϕ_g, at the glass transition temperature. We calculate $\phi_{g1} = 0.70$ and $\phi_{g2} = 0.80$. At the glass transition, a fraction, $1 - \phi_{gi}$, of volume is "unoccupied". However, this volume makes a negligibly small contribution to the mobility of the molecules over experimental time scales. Because the particles are tightly localized, a redistribution of the volume $1 - \phi_{gi}$ would require a significant energy penalty, such as an overlap of particle volumes.[39] The volume $1 - \phi_{gi}$ is therefore "immobilized". The "immobilized" volume fraction is distinct from the fractional free volume, $\phi_{gi} - \phi_i$. The distinction between the three types of volume, free, immobilized, and occupied, is critical to the extension of the CS equation to two components.

In modeling the mixtures of CA and EtOH we use an equation of state that is an extension of the Carnahan−Starling equation for mixtures[53]

$$\frac{p_{CSm}}{k_B T} = \frac{n_0}{1 - n_3} + \frac{n_1 n_2 (1 + (1/3) n_3^2)}{(1 - n_3)^2} + \frac{n_2^3 (1 - (2/3) n_3 + (1/3) n_3^2)}{12\pi (1 - n_3)^3} \quad (20)$$

dx.doi.org/10.1021/jp1120838 |J. Phys. Chem. B 2011, 115, 3981–3991

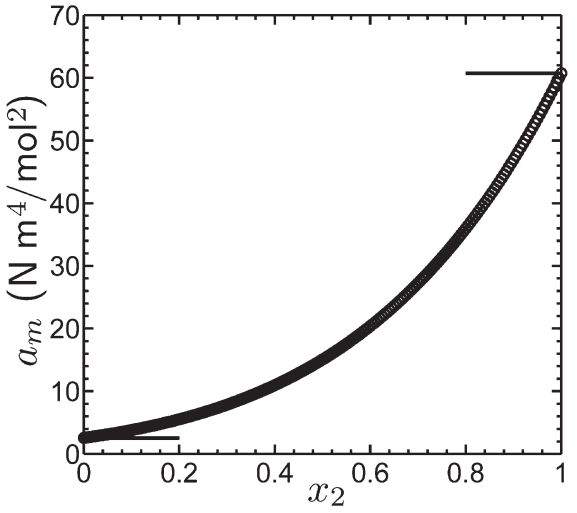

Figure 5. As x_2 varies from 0 to 1, $a_m = a_m'N_a^2$ varies continuously between $a_1 = a_1'N_a^2$ and $a_2 = a_2'N_a^2$. Values of a_1 and a_2 are shown by the horizontal lines.

where p_{CSm} is the total or hard-sphere pressure of the mixture, $p_{CSm} = p_{atm} + a_m'\bar{\rho}_m^2 = p_{atm} + a_m'(\bar{\rho}_1 + \bar{\rho}_2)^2$. The parameter a_m' characterizes the attractions in the mixture, and $\bar{\rho}_i$ is the number density of particles of component i. The parameters n_0, n_1, n_2, and n_3 are given by

$$n_0 = \sum_i \bar{\rho}_i,\ n_1 = \sum_i \bar{\rho}_i r_i^*,\ n_2 = \sum_i \bar{\rho}_i a_i^*,\ n_3 = \sum_i \bar{\rho}_i v_i^* \quad (21)$$

where $a_i^* = 4\pi r_i^{*2}$ and $v_i^* = (4/3)\pi r_i^{*3}$.

To be consistent with our density measurements showing ideal mixing, we require the volume per molecule of the mixture, $v_m = 1/\rho_m$, to depend on the molecular volumes, v_i, of the single components at the same temperature and pressure

$$v_m = x_1 v_1 + x_2 v_2 \quad (22)$$

This relation is only assumed to be valid at 20 °C. For a given x_2, we first calculate v_m by assuming ideal mixing. This value is then used in the two-component equation of state to calculate the total pressure, p_{CSm}, from which we calculate the van der Waals parameter, a_m', using the relation $p_{CSm} = p_{atm} + a_m'/v_m^2$. Values of a_m' depend on x_2 and vary continuously between the single-component values a_1' and a_2' as x_2 varies from 0 to 1 (Figure 5). We assume that values of a_m' do not depend on temperature or pressure. Although we only enforce ideal mixing at 20 °C, the equation of state predicts values of v_m that are within a few percent of ideal mixing values over a wide range of temperatures. Therefore, our model does not significantly depend on the fact that the ideal volume of mixing is imposed only at 20 °C.

Calculations of T_{gm} of the mixture require knowledge of the combined volume fraction, ϕ_{gm}, at which the glass transition will occur for each value of x_2. Values of ϕ_{gm} are determined by assuming that both the immobilized and the free volume mix in an ideal manner. We define a ratio of immobilized to occupied volume at T_{gi} for the single component, $s_i = (1 - \phi_{gi})/\phi_{gi}$. The glass transition of the single component occurs at the molecular volume $v_{gi} = v_i^*(1+s_i)$. We assume that the glass transition of the mixture occurs at a molecular volume $v_{gm} = x_1 v_1^*(1 + s_1) + x_2 v_2^*(1 + s_2)$. Values of T_{gm} predicted using this relation are in good agreement with those predicted using the Gordon−Taylor equation, eq 10, with the maximum error less than 11% (see

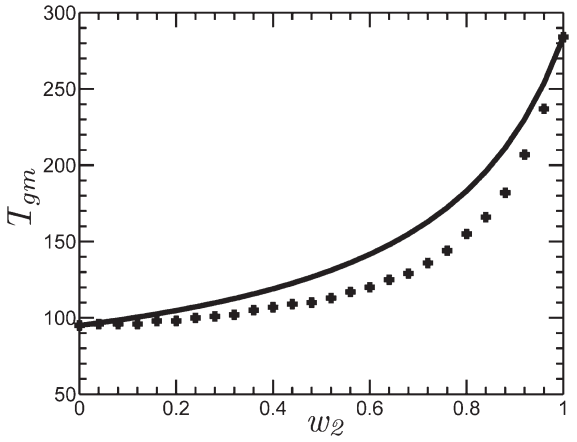

Figure 6. Symbols show values of T_{gm} calculated from the two-component equation of state. The solid line shows T_{gm} predicted with the Gordon−Taylor equation, eq 10.

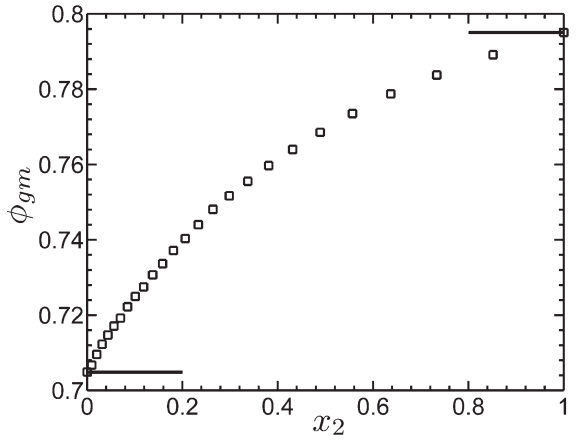

Figure 7. Predicted values, ϕ_{gm}, of the glass transition volume fraction. Horizontal lines correspond to values of ϕ_{gi} predicted by the CS−vdW for single components.

Figure 6). Values of the volume fraction, ϕ_{gm}, at T_g interpolate smoothly between values of ϕ_{g1} and ϕ_{g2} (see Figure 7).

Knowledge of ϕ_{gm} allows us to calculate the fractional free volume of the mixture, $\phi_{gm} - \phi_m$, for a given concentration of CA. As expected, the self-diffusivity collapses to a single function when it is plotted as a function of $v_m^*/v_{fm} = \phi_m/(\phi_{gm} - \phi_m)$, Figure 8. This plot is obtained with no adjustable parameters; values of v_m^* and v_{fm} were calculated only from literature values of r_{vdw}, ρ, M_w, T_g, the CS−vdW equation of state, and it is modified form for two components.

As suggested by the form of the elementary free volume model, we seek to model the system as an effective single component using the single-component CS−vdW equation of state. The particle size of the effective single-component system is given by v_m^*, and the strength of attraction is given by a_m. The CS−vdW equation of state is used to calculate the volume fraction, ϕ_{ES}, of the effective single-component system as x_2 and T are varied. The measured diffusivities collapse when plotted as a function of $\phi_{ES}/(\phi_{gm} - \phi_{ES})$ (see Figure 9).

We expect that values of $\phi_m/(\phi_{gm} - \phi_m)$ and $\phi_{ES}/(\phi_{gm} - \phi_{ES})$ should be similar to values of v_m^*/v_{fm} calculated using the linear extrapolation of the coefficient of thermal expansion (eq 8

dx.doi.org/10.1021/jp1120838 |J. Phys. Chem. B 2011, 115, 3981–3991

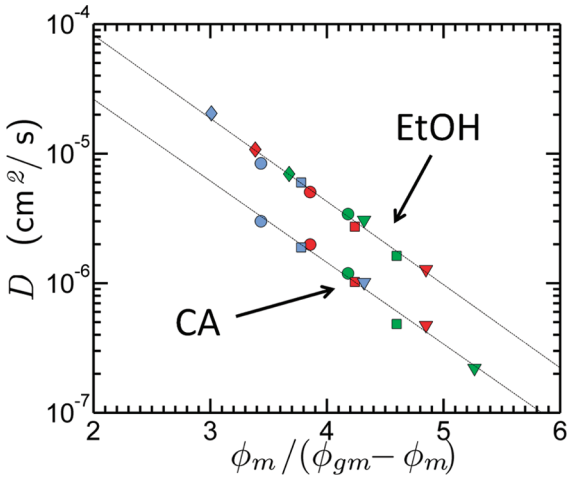

Figure 8. Measured values of self-diffusivity collapse when plotted as a function of $\phi_m/(\phi_{gm} - \phi_m)$, where ϕ_m is the combined volume fraction of the mixture. It is calculated from an extension of the CS−vdW equation of state to two components.[53] The solid lines are fits to eq 5. The symbols near the upper line pertain to EtOH, and the symbols near the lower line pertain to CA. Symbols are the same as those used in Figure 2: T = 50 (blue symbols), 25 (red symbols), and 9 °C (green symbols); w_2 = 0 (diamonds), 0.2 (circles), 0.3 (squares), and 0.4 (triangles).

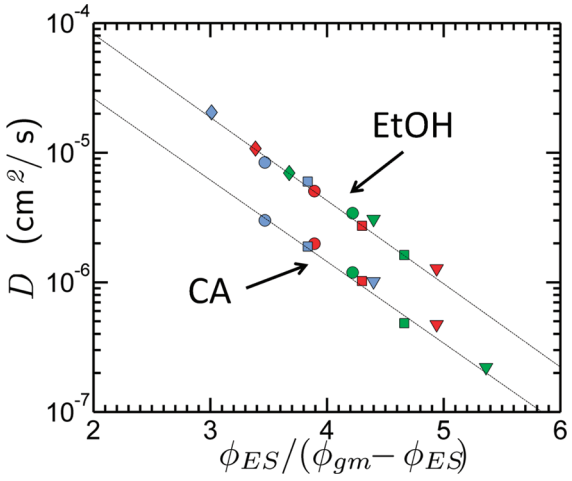

Figure 9. Measured values of self-diffusivity collapse when plotted as a function of $\phi_{ES}/(\phi_{gm} - \phi_{ES})$, where ϕ_{ES} is the volume fraction of the effective single component. It is calculated from the CS−vdW equation of state for a single component of size v_m^*. The solid lines are fits to eq 5. The symbols near the upper line pertain to EtOH, and the symbols near the lower line pertain to CA. Symbols are the same as those used in Figure 2: T = 50 (blue symbols), 25 (red symbols), and 9 °C (green symbols); w_2 = 0 (diamonds), 0.2 (circles), 0.3 (squares), and 0.4 (triangles).

and Figure 3). However, the values of v_m^*/v_{fm} are somewhat lower because they were generated by arbitrarily assigning $p = p_1 = p_2 = 0.7$. The ratio of the thermal expansion coefficient, α_{CS1}, from the CS−vdW equation of state to α_1, suggests $p = \alpha_{CS1}/\alpha_1 = 0.81$. When this value of p is used with eq 8, then calculated values of v_m^*/v_{fm} show excellent agreement with values of $\phi_m/(\phi_{gm} - \phi_m)$ and $\phi_{ES}/(\phi_{gm} - \phi_{ES})$ calculated using the equations of state.

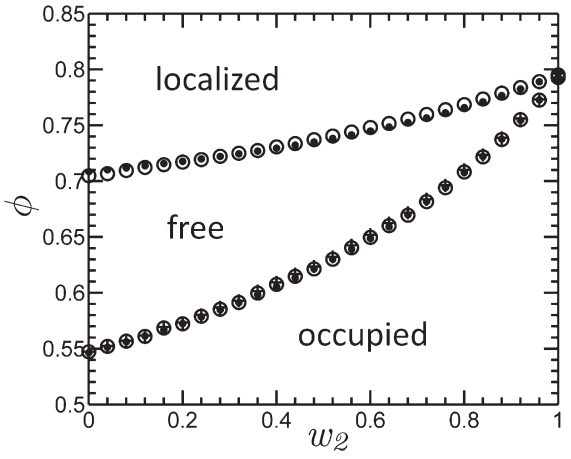

Figure 10. Distribution of the total volume into "occupied", "free", and "localized" volume at STP. Volume distributions are calculated using three approaches, as described in the text. In the first approach, shown by filled circles, the free volume, v_{fm}, is calculated from eq 8 and the occupied volume v_m^* is calculated from eq 4. These are normalized by the total volume per molecule, v, and the remaining volume is attributed to "localized" volume. Volume distributions are also calculated using the two-component equation of state (open circles) and the single-component CS−vdW equation of state for an effective single component (crosses). The symbols between the "free" and the "occupied" regions correspond to values of the combined volume fraction, ϕ_m. The symbols at the boundary between the "free" and the "localized" regions correspond to values of ϕ_g. These values are taken to be the same for both the two-component and the single-component equations of state.

Combining our calculations of v_{fm} from eq 8, v from density measurements, and v_m^* we determine the distribution of the total volume between "occupied", "free", and "localized" volume as a function of x_2 at STP (filled circles in Figure 10). These values show excellent agreement with the same distributions calculated using both the two-component equation of state and the single-component equations of state (open circles and crosses, respectively, in Figure 10). In this plot, the increase in ϕ_{gm} with w_2 corresponds to a decrease in the "localized" free volume, $1 - \phi_{gm}$, shown in the upper portion of the plot. The increase in ϕ_{gm} would, by itself, tend to favor more mobility by allowing for a more efficient packing of the particles. However, this effect is offset by increases in v_m^* and a_m' as w_2 increases. The increase in v_m^* tends to decrease the entropic stress, k_BT/v_m^*, and the increase in a_m' tends to increase the effective pressure, p_{eff}. Both of these effects cause the combined volume fraction, ϕ_m, to increase, thereby driving the free volume, $\phi_{gm} - \phi_m$, to lower values and favoring more solid-like behavior.

The development of the Gordon−Taylor relationship (eq 9) from the elementary free volume equation required the assumption that the system could be modeled using the Simha−Boyer rule (eq 12). With the equation of state approach this assumption is not necessary. Using the equation of state, we find that values of $\alpha_{CS1}T_{g1}$ and $\alpha_{CS2}T_{g2}$ at 20 °C and atmospheric pressure are within 16% of each other, in rough agreement with the Simha−Boyer rule. We also use the equation of state to calculate values of the thermal expansion coefficient, α_{CSm}, of the mixture as a function of x_2 at STP. These values smoothly interpolate between the values of α_{CS1} and α_{CS2}, as shown by the black squares in Figure 11. According to eq 18, the thermal expansion coefficient of the mixture can be predicted from T_{gm} using the

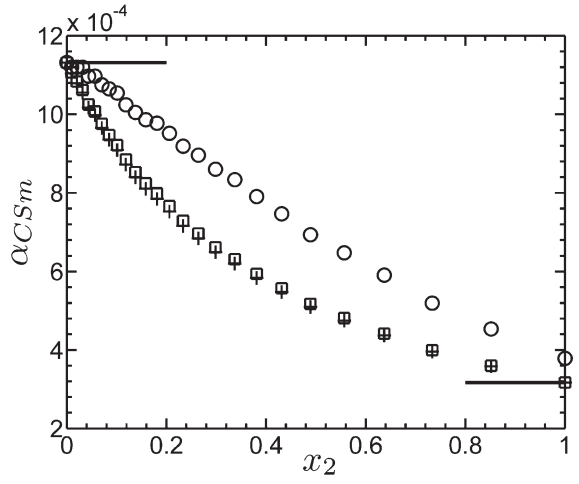

Figure 11. Calculation of the thermal expansion coefficient, α_{CSm}, of the mixture using the two-component equation of state (squares) agrees with calculations of the thermal expansion of the effective single component, calculated using the CS−vdW equation of state (crosses). Estimates of the thermal expansion coefficient of the effective single component (eq 18) are shown by the circles. The coefficients of the thermal expansion of the single components, α_{CSi}, calculated using the CS−vdW equation of state, are shown by the horizontal lines.

Simha−Boyer rule. We test this prediction estimating values of α_{CSm} through the relation $(\alpha_{CS1}T_{g1})/T_{gm}$, shown by the circles in Figure 11. This prediction shows fair agreement with the predictions from the two-component equation of state, with the maximum error of 35%. Calculations of the coefficient of thermal expansion for the effective single-component liquid show excellent agreement with values of the coefficient of thermal expansion for the mixtures (see the crosses in Figure 11). This provides additional validation that the two-component mixture can be mapped to an effective single component.

IV. DISCUSSION

We demonstrated that the concentration-induced transition to slower dynamics in a two-component system can be mapped to an effective single component. We began by estimating values of v_m^*, v_{fm}, and T_{gm} associated with the mixtures. By plotting the self-diffusivity as functions of these variables we are able to collapse both the temperature and the concentration dependence of the self-diffusivity onto master curves.

This general approach has been used in other systems. For example, T_{gm} has been measured at various concentrations of trehalose and borax in both aqueous trehalose solutions and aqueous trehalose/borax solutions. Viscosities measured at different concentrations and temperatures collapsed to a single curve when plotted as a function of T/T_{gm}, and the functional form was fit using standard equations for single-component systems.[54]

Rather than simply applying single-component models to our mixture data, we analyzed our system using both single- and two-component models. We used a two-component version of the CS−vdW equation to calculate how the occupied volume, free volume, and localized volumes depend on the relative concentration of the two components. This information was used with the Doolittle equation to predict self-diffusivity. We then showed that the same distributions of volume can be calculated by treating the mixture as an effective single component. This is possible despite the fact that the two components exhibited significant differences in v^*, T_g, ϕ_g, and a'. The effective single component exhibits values of v_m^*, T_{gm}, ϕ_{gm}, and $a_m{}'$ that are intermediate to respective values of the single components.

Despite the success of this model, we expect that the CS−vdW approach will exhibit significant limitations in modeling dynamical effects. Simulations indicate that replacement of molecular attractions with an effective pressure can approximately describe the dynamics of liquids at sufficiently high temperature but will fail for viscous liquids.[55] Therefore, we expect that to model data in which the T is sufficiently close to T_{gm}, it may be necessary to employ an alternative model, such as mode coupling theory. However, even in the more viscous regime, the effective single-component approach may still be appropriate: this is suggested by the collapse of the aqueous trehalose solution and the aqueous trehalose/borax solution data in terms of T_{gm} even in the viscous regime where $T_{gm} < T < 1.2T_{gm}$.[54]

One reason that the elementary free volume approach can be used to model our system is that it exhibits ideal mixing. For hard spheres, ideal mixing is expected for size ratios in the range of $0.7 < q < 1.0$. Our system is different from hard spheres because the two phases exhibit different values of ϕ_g. Nevertheless, our system qualitatively resembles the hard-sphere system for which $0.7 < q < 1.0$, because the dynamics of each phase depend on the common free volume. The fact that $q = 0.71$ for our system suggests that it is close to the limit where these idealized properties will break down: systems of smaller size ratio may not exhibit ideal mixing, and the dynamics of both systems may not depend on a common free volume. However, this does not necessarily preclude the possibility that the system can be treated as an effective single component.

Indeed, the approach of defining an effective single component is routinely used in the limit of small q, which corresponds to colloidal systems. In this case, colloids are treated as if in a viscous continuum: both the "occupied" and the "unoccupied" volume of the solvent act as "unoccupied" volume with respect to the colloidal phase. The phase behavior of colloidal systems can be modeled by assuming that the only function of the solvent is to provide the confining volume to the colloidal particles and to modify the effective mean force between particles.[19,56] Therefore, in the limit that $q \ll 1.0$, the volume fraction of the effective single component is typically designated to be the volume fraction, ϕ_2, of the large particles. By contrast, in our approach, the volume fraction of the effective single component is taken to be $\phi_m = \phi_1 + \phi_2$. On the basis of a comparison to hard spheres, we expect that this approach is appropriate for $0.7 < q < 1.0$. This implies that as q varies continuously from 0.7 to $\ll$1.0, the contribution of the small particles to the volume fraction of the effective single component may continuously decrease from ϕ_1 to zero.

Clarification of these issues is complicated by the fact that schemes for identifying effective single components may not be unique. For example, the approach of assigning the effective single-component volume fraction to be ϕ_2 has been applied to binary systems over a wide range of q from $q \ll 1.0$ to $q = 1.0$.[19] This approach has been used to predict how the equilibrium transition from a liquid to a crystalline state depends on the relative concentration of the two species. However, we expect that the approach presented here is more useful for describing dynamical transitions due to particle crowding associated with the formation of a double glass the region near $q \approx 1$.

A second advantage of our approach is that it is well suited for using mixtures to provide an experimental approximation of an approach to the glass transition that is not easily realized in a physical experiment: a continuous transition in the material properties of a single component. Such a transition can occur at constant pressure and temperature when the size or strength of the attractions are continuously modified. In the case of the CA/EtOH system, the "property-dependent" transition of the effective single component corresponds to a continuous increase in the properties of the effective single component, ϕ_{gm}, v_m^*, and a_m'.

The concentration-induced increase in ϕ_{gm} tends to favor more efficient particle packing, thereby potentially increasing the total available free volume, $\phi_{gm} - \phi_m$. However, increasing the concentration of CA also causes the entropic stress, kT/v_m^*, to decrease, and this tends to reduce the free volume and drive the particles to a more solid-like state. Increasing the concentration of CA also causes a_m' to increase, thereby further reducing the free volume. These two effects dominate any potential increase in free volume due to the increase in ϕ_{gm}, and the net effect of an increase in the concentration of CA is to cause the system to become more solid-like. Because these effects modify the dynamics of the mixture through the free volume, they can be described, together with the effect of temperature, in terms of a simple free volume model of a single component.

V. CONCLUSIONS

We characterized the dynamics of a molecular system that exhibits a concentration-induced transition from a liquid to a glassy state at constant temperature and pressure. We modeled the dependence of the self-diffusivity of both CA and EtOH on the concentration and temperature by using a free volume approach and have shown that a concentration-induced approach to glassy dynamics can be mapped onto continuous changes in the properties of an effective single-component system. Because of this mapping, we expect that studies of molecular mixtures can yield fundamental insights into how material properties, such T_g, and ϕ_g, depend on molecular parameters, including the strength of attraction and the particle size.

Understanding the effect of particle size on glassy dynamics is particularly important for elucidating the differences and similarities between molecular and colloidal systems. Although our study is performed on a molecular system, the concentration-induced transition to glassy behavior exhibited by the CA/EtOH system is reminiscent of the concentration-induced glass transition exhibited by colloidal systems. In colloidal systems, the colloidal particles are usually sufficiently large such that the granular of nature of the solvent can be ignored and the colloidal phase can be treated as an effective single component. Our results show that as the "colloidal" particle approaches the size of the solvent molecule, the granular nature of the solvent molecules modifies the dynamics of the system, because they effectively crowd the larger particles.

Nevertheless, even in this limit, the molecular mixture can be treated as an effective single-component system where the particle size of the effective single component is the number-averaged size of the two particle sizes in the mixture. By studying the dynamics of mixtures, it is therefore possible to develop a better understanding of how variations in molecular size effect both the phase behavior and the dynamics. Further clarification of these relationships will strengthen our understanding of phase behavior in large molecules, or nanoparticles, that are intermediate between molecular and colloidal systems.

AUTHOR INFORMATION

Corresponding Author
*E-mail: larsen@illinois.edu.

ACKNOWLEDGMENT

This work was performed under Award No. DEFG02-91-ER45439 from the U.S. Department of Energy, University of Illinois at Urbana−Champaign.

REFERENCES

(1) Zaccarelli, E. *J. Phys.: Condens. Matter* **2007**, *19*, 323101.1–323101.50.
(2) Sciortino, F. *Eur. Phys. J. B* **2008**, *64*, 505–509.
(3) Mattsson, J.; Wyss, H. M.; Fernandez-Nieves, A.; Miyazaki, K.; Hu, Z.; Reichman, D. R.; Weitz, D. A. *Nature* **2009**, *462*, 83–86.
(4) Corezzi, S.; Capaccioli, S.; Casalini, R.; Fioretto, D.; Paluch, M.; Rolla, P. A. *Chem. Phys. Lett.* **2000**, *320*, 113–117.
(5) Li, G.; King, H. E., Jr.; Oliver, W. F.; Herbst, C. A.; Cummins, H. Z. *Phys. Rev. Lett.* **1995**, *74*, 2280–2283.
(6) Voigtmann, T. *Phys. Rev. Lett.* **2008**, *101*, 095701.1–095701.4.
(7) Pusey, P. N.; Vanmegen, W. *Nature* **1986**, *320*, 340–342.
(8) Vanmegen, W.; Underwood, S. M. *Phys. Rev. Lett.* **1993**, *70*, 2766–2769.
(9) Hancock, B. C.; Zografi, G. *Pharm. Res.* **1994**, *11*, 471–477.
(10) Jaya, S.; Das, H. *Food Bioprocess Technol.* **2009**, *2*, 89–95.
(11) Kelley, F. N.; Bueche, F. *J. Polym. Sci.* **1961**, *50*, 549–556.
(12) Mackay, M. E.; Dao, T. T.; Tuteja, A.; Ho, D. L.; Van Horn, B.; Kim, H. C.; Hawker, C. J. *Nat. Mater.* **2003**, *2*, 762–766.
(13) He, G.; Tan, R. B. H.; Kenis, P. J. A.; Zukoski, C. F. *J. Phys. Chem. B* **2007**, *111*, 14121–14129.
(14) de Loos, M.; Feringa, B. L.; van Esch, J. H. *Eur. J. Org. Chem.* **2005**, 3615–3631.
(15) Germain, P.; Amokrane, S. *Phys. Rev. Lett.* **2009**, *102*, 058301.1–058301.4.
(16) Williams, S. R.; van Megen, W. *Phys. Rev. E* **2001**, *64*, 041502–1−041502−9.
(17) Imhof, A.; Dhont, J. K. G. *Phys. Rev. Lett.* **1995**, *75*, 1662–1665.
(18) Waziri, S. M.; Hamad, E. Z. *Ind. Eng. Chem. Res.* **2006**, *45*, 7251–7255.
(19) Dijkstra, M.; van Roij, R.; Evans, R. *Phys. Rev. E* **1999**, *59*, 5744–5771.
(20) Gotze, W.; Voightman, Th. *Phys. Rev. E* **2003**, *67*, 021502.1–021502.14.
(21) Schweizer, K. S. *J. Chem. Phys.* **2007**, *127*, 164506−1–164506−9.
(22) Brambilla, G.; El Masri, D.; Pierno, M.; Berthier, L.; Cipelletti, L.; Petekidis, G.; Schofield, A. B. *Phys. Rev. Lett.* **2009**, *102*, 085703.1–085703.4.
(23) Lemaignan, C. *Acta Metall.* **1980**, *28*, 1657–1661.
(24) Lu, Q.; Zografi, G. *J. Pharm. Sci.* **1997**, *86*, 1374–1378.
(25) Privalko, V. P. *J. Phys. Chem.* **1980**, *84*, 3307–3312.
(26) Gordon, M.; Taylor, J. S. *J. Appl. Chem.* **1952**, *2*, 493–500.
(27) Carnahan, N. F.; Starling, K. E. *J. Chem. Phys.* **1969**, *51*, 635–636.
(28) Ben-Amotz, D.; Herschbach, D. R. *J. Phys. Chem.* **1990**, *94*, 1038–1047.
(29) In *CRC Handbook of Chemistry and Physics*, 88th ed. (Internet Version 2008);Lide, D. R., Ed.; CRC Press/Taylor and Francis: Boca Raton, FL, 2008.
(30) Stejskal, E. O.; Tanner, J. E. *J. Chem. Phys.* **1965**, *42*, 288–292.

(31) Callaghan, P. T. *Principles of Nuclear Magnetic Resonance Microscopy*; Oxford University Press: Oxford, 1991.
(32) Tanner, J. E. *J. Chem. Phys.* **1970**, *52*, 2523–2526.
(33) Holz, M.; Heil, S. R.; Sacco, A. *Phys. Chem. Chem. Phys.* **2000**, *2*, 4740–4742.
(34) Stilbs, P. *Prog. Nucl. Magn. Reson. Spectrosc.* **1987**, *19*, 1–45.
(35) Edward, J. T. *J. Chem. Educ.* **1970**, *47*, 261–270.
(36) Bondi, A. *J. Phys. Chem.* **1964**, *68*, 441–451.
(37) Angell, C. A.; Ngai, K. L.; McKenna, G. B.; McMillan, P. F.; Martin, S. W. *J. Appl. Phys.* **2000**, *88*, 3113–3157.
(38) Larson, R. G. *The Structure and Rheology of Complex Fluids*; Oxford University Press: New York, 1999.
(39) Debenedetti, P. G. *Metastable Liquids: Concepts and Principles*; Princeton University Press: Princeton, NJ, 1996.
(40) Cohen, M. H.; D. Turnbull, D. *J. Chem. Phys.* **1959**, *31*, 1164–1169.
(41) Boned, C.; Allal, A.; Baylaucq, A.; Zeberg-Mikkelsen, C. K.; Bessieres, D.; Quinones-Cisneros, S. E. *Phys. Rev. E* **2004**, *69*, 031203−1–031203.6.
(42) Rah, K.; Eu, B. C. *J. Chem. Phys.* **2001**, *115*, 2634–2640.
(43) Cohen, M. H.; Grest, G. S. *Phys. Rev. B* **1979**, *20*, 1077–1098.
(44) Doolittle, A. K. *J. Appl. Phys.* **1951**, *22*, 1471–1475.
(45) Vrentas, J. S.; Duda, J. L.; Ling, H. C. *J. Polym. Sci., Polym. Phys.* **1985**, *23*, 275–288.
(46) Guo, C. J.; De Kee, D. *Chem. Eng. Sci.* **1991**, *46*, 2133–2141.
(47) Guo, C. J.; De Kee, D. *Polym. Eng. Sci.* **1996**, *35*, 78–83.
(48) Wesselingh, J. A.; Bollen, A. M. *Chem. Eng. Res. Des.* **1997**, *75*, 590–602.
(49) Rah, K.; Eu, B. C. *J. Chem. Phys.* **2002**, *116*, 7967–7976.
(50) Simha, R.; Boyer, R. F. *J. Chem. Phys.* **1962**, *37*, 1003–1007.
(51) Jaeger, H. M.; Nagel, S. R. *Science* **1992**, *255*, 1523–1531.
(52) Donev, A.; Cisse, I.; Sachs, D.; Variano, E. A.; Stillinger, F. H.; Connelly, R.; Torquato, S.; Chaikin, P. M. *Science* **2004**, *303*, 990–993.
(53) Hansen-Goos, H.; Roth, R. *J. Chem. Phys.* **2006**, *124*, 154506.1–154506.8.
(54) Miller, D. P.; de Pablo, J. J.; Corti, H. R. *J. Phys. Chem. B* **1999**, *103*, 10243–10249.
(55) Berthier, L.; Tarjus, G. *Phys. Rev. Lett.* **2009**, *103*, 170601.1–170601.1.
(56) Dijkstra, M.; van Roij, R.; Evans, R. *J. Chem. Phys.* **2000**, *113*, 4799–4809.